

## The Interaction of 14-Mev Neutrons with Protons and Deuterons\*

J. C. ALLRED, A. H. ARMSTRONG,† AND L. ROSEN

University of California, Los Alamos Scientific Laboratory, Los Alamos, New Mexico

(Received January 12, 1953)

Nuclear emulsions in conjunction with a neutron collimator have been used to measure the differential cross section as a function of angle for the elastic scattering of monoenergetic 14-Mev neutrons by protons and by deuterons. Measurements were carried out in the angular regions corresponding to neutrons being scattered at angles between  $48^\circ$  and  $154.5^\circ$  in the center-of-mass system by protons and between  $46^\circ$  and  $176^\circ$  in the same coordinate system by deuterons. The  $n$ - $p$  scattering data are consistent with isotropic scattering in the center-of-mass system, and are in excellent agreement with the data of Barschall and Taschek. The  $n$ - $d$  elastic scattering data are strongly anisotropic. The shape of the angular distribution of the neutrons elastically scattered by deuterons may be inferred from the differential cross sections in millibarns for the following laboratory angles:  $2^\circ$ ,  $435 \pm 28$ ;  $10^\circ$ ,  $342 \pm 27$ ;  $20^\circ$ ,  $78 \pm 9.3$ ;  $30^\circ$ ,  $38 \pm 4.2$ ;  $40^\circ$ ,  $59 \pm 5.2$ ;  $50^\circ$ ,  $104 \pm 9.0$ ;  $60^\circ$ ,  $136 \pm 12$ ;  $65^\circ$ ,  $142 \pm 14$ . Strong evidence for the reaction  $D(n, 2n)H^2$  has been found and an attempt to determine the energy and angular distribution of the disintegration protons was moderately successful.

### I. INTRODUCTION

THE extensive theoretical calculations which have already been carried out on the scattering of fast neutrons by protons and deuterons are a good indication of the importance attached to these two reactions in the eventual understanding of the nature of nuclear forces.

Most theories<sup>1</sup> dealing with the interaction between neutrons and protons predict spherically symmetric scattering below 10-Mev neutron energy and this is indeed well borne out by all recent experiments.<sup>2</sup> For energies above 10 Mev, however, appreciable deviations from symmetry are predicted, depending upon the nature of the forces assumed for the neutron-proton interaction. Although angular distribution measurements<sup>3</sup> at incident neutron energies between 10 and 15 Mev have not all been in good agreement, the most recent such measurements are consistent with spherical symmetry to within approximately 5 percent. In the study of  $n$ - $p$  scattering there is some advantage to be gained in not using neutron energies much in excess of 14 Mev, since for high neutron energies the analysis is complicated by the presence of nonzero angular momentum states as well as relativistic effects.

Calculations by Buckingham and Massey<sup>4</sup> on the neutron-deuteron collision up to 11.5-Mev neutron

energy have recently been extended by Buckingham, Hubbard, and Massey<sup>5</sup> to include neutron energies up to 16 Mev. Here, also, the theoretical predictions concerning the angular distribution of the neutrons elastically scattered by deuterons show a marked dependence on the type of nuclear force assumed. From a comparison of their theoretical results with available experimental data, these authors conclude that the experimental evidence is consistent with the equivalence of  $n$ - $n$  and  $p$ - $p$  forces at the energies involved and that the symmetrical exchange type forces are favored over ordinary forces. Gordon and Barfield<sup>6</sup> arrived at somewhat the same conclusions from their phase shift analysis of low energy  $n$ - $d$  scattering data in which they showed that  $d$ -waves are significant at 4.5 and 5.5 Mev.

Latter and Latter<sup>7</sup> made phase shift analyses of both  $p$ - $d$  and  $n$ - $d$  elastic scattering data for incident neutron and proton energies below 5.5 Mev. From a comparison of Wantuch's<sup>8</sup>  $n$ - $d$  angular distributions at 4.5 and 5.5 Mev with the  $p$ - $d$  angular distributions of Rosen and Allred<sup>9</sup> at 10.4-Mev incident deuteron energy, they conclude that these experimental data are consistent with the principle of charge independence of nuclear forces. This conclusion agrees with that previously arrived at by Breit<sup>10</sup> from a consideration of the same data.

The  $n$ - $d$  problem is complicated by two features which do not arise in the  $n$ - $p$  interaction below 14 Mev. In the first place, the angular distribution in the center-of-mass system is strongly anisotropic. Therefore, unless measurements can be made over the entire angular region ( $0^\circ$  to  $180^\circ$  in the center-of-mass system), which has so far not been done, it is quite

\* Work performed under the auspices of the U. S. Atomic Energy Commission.

† Now at Wellesley College, Wellesley, Massachusetts.

<sup>1</sup> W. Pauli, *Meson Theory of Nuclear Forces* (Interscience Publishers, Inc., New York, 1946), p. 55.

<sup>2</sup> L. Rosenfeld, *Nuclear Forces* (Interscience Publishers, Inc., New York, 1948) Vol. 1, p. 123.

<sup>3</sup> Amaldi, Bocciaelli, Ferretti, and Trabacchi, *Naturwiss.* **30**, 582 (1942); F. C. Champion and C. F. Powell, *Proc. Roy. Soc. (London)* **A183**, 64 (1944); C. F. Powell and G. P. S. Occhialini, *Fundamental Particles* (The Physical Society, London, 1947), p. 150. G. Wentzel, *Revs. Modern Phys.* **19**, 10 (1947), footnote 38; J. S. Laughlin and P. G. Kruger, *Phys. Rev.* **73**, 197 (1948); H. H. Barschall and R. F. Taschek, *Phys. Rev.* **75**, 1819 (1949); W. G. Cross, *Phys. Rev.* **87**, 223 (1952).

<sup>4</sup> R. A. Buckingham and H. S. W. Massey, *Proc. Roy. Soc. (London)* **A179**, 123 (1941); H. S. W. Massey and R. A. Buckingham, *Phys. Rev.* **71**, 558 (1947).

<sup>5</sup> Buckingham, Hubbard, and Massey, *Proc. Roy. Soc. (London)* **A211**, 183 (1952).

<sup>6</sup> M. M. Gordon and W. D. Barfield, *Phys. Rev.* **86**, 679 (1952).

<sup>7</sup> A. L. Latter and R. Latter, *Phys. Rev.* **86**, 727 (1952).

<sup>8</sup> E. Wantuch, *Phys. Rev.* **79**, 729 (1950).

<sup>9</sup> L. Rosen and J. C. Allred, *Phys. Rev.* **82**, 777 (1951).

<sup>10</sup> G. Breit, *Phys. Rev.* **80**, 1110 (1950).

essential that absolute differential cross sections be measured with high precision. In the second place it is energetically possible for the deuteron to disintegrate upon impact with a neutron having an incident energy above 3.3 Mev. To determine the energy and angular distribution of the emitted protons and the total cross section for deuteron breakup is in itself an interesting and challenging problem which has thus far not been resolved for the energy region under consideration. Furthermore, in order to evaluate the absolute, or even the relative, differential cross section for elastic scattering, it is quite essential that account be taken of the inelastic cross section. This problem is especially troublesome in the angular region where the elastic scattering cross section goes through a minimum.

Angular distribution data for  $n$ - $d$  elastic scattering have been published for various energies from 1.5 Mev to 14 Mev.<sup>8,11</sup> Most of these data fall into a fairly consistent pattern. However, where two or more investigators have reported detailed results for the same neutron energy, the quantitative agreement is often somewhat less than adequate from the standpoint of theoretical interpretation.<sup>5</sup> This situation may be expected to change with the increasing availability of more intense and more nearly monoenergetic neutron sources.

A universal difficulty in almost all neutron experiments involving the measurement of differential cross sections is the lack of adequate neutron intensity. This limitation follows from the fact that the neutrons must themselves be produced in a nuclear reaction. It is therefore usually the case that one must either sacrifice angular resolution to permit the detector to subtend a relatively large solid angle or "make do" with relatively few angles and poor statistical accuracy. In order partially to circumvent these difficulties we have used nuclear plates in a manner which has the following advantages.

(a) Data in the laboratory angular region  $10^\circ$  to  $170^\circ$  are taken simultaneously during a given run. The relative accuracy of the differential cross sections is thus improved, since inaccuracies involved in the absolute measurement of the neutron flux enter alike for each angle.

(b) Nuclear emulsions enable one to establish the directions in space for the particles recorded and one can divide the plates into small areas whose relation in space to the target is accurately known. It is therefore

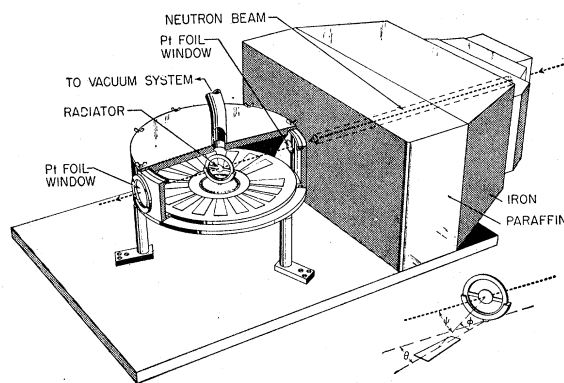


FIG. 1. Perspective drawing of neutron collimator and multiplate camera.

possible to arrange the detectors so that they subtend rather large angles at the target without undue loss of angular or energy resolution.

(c) The solid angles subtended at the target by the detector areas analyzed were determined from the orientation of the plates with respect to the target. Determination of these angles was made possible by accurate positioning of the plates and there was no need for defining slits. Thus possible difficulties due to slit edge penetration and scattering were eliminated.

## II. EXPERIMENTAL METHOD

The experimental arrangement is shown in Fig. 1. The source of neutrons for this experiment was the  $T(d, n)He^4$  reaction. The accelerator used was the Los Alamos Cockcroft-Walton set from which the molecular beam of 250-kev deuterons is magnetically analyzed, collimated through a  $\frac{1}{4}$ -in. diaphragm and intercepted by a thick zirconium-tritium target. The plane of the target makes an angle of  $45^\circ$  with the deuteron beam direction. The tritium is absorbed in a zirconium film which is deposited on a thin tungsten disk.<sup>12</sup> The axis of the neutron collimator (Fig. 1) formed an angle of very nearly  $90^\circ$  with the deuteron beam, the mean neutron energy in this direction being  $14.1 \pm 0.1$  Mev. The intersection of the Zr-T target area with the deuteron beam formed an ellipse of which the largest projected dimension along the collimator axis was  $\frac{3}{8}$  in. The neutrons were monitored by counting a known fraction of the alphas from the above reaction by means of a proportional counter mounted 22 in. from the target in a geometry permitting a view of the entire target area.<sup>13</sup>

The neutron collimator has two components. The 18-in. section nearest the source is made of iron and has a  $\frac{3}{4}$ -in. diameter circular channel along its axis.

<sup>12</sup> Graves, Rodriguez, Goldblatt, and Meyer, *Rev. Sci. Instr.* **20**, 579 (1949).

<sup>13</sup> We are indebted to J. H. Coon for making available to us the Cockcroft-Walton source and the auxiliary equipment required to produce and monitor precisely the neutrons used in these experiments, and for his generous assistance.

<sup>11</sup> Kruger, Shoupp, and Stallman, *Phys. Rev.* **52**, 678 (1937); H. H. Barschall and M. H. Kanner, *Phys. Rev.* **58**, 590 (1940); Coon, Davis, and Barschall, *Phys. Rev.* **70**, 104 (1946); J. H. Coon and H. H. Barschall, *Phys. Rev.* **70**, 592 (1946); J. F. Darby and J. B. Swan, *Nature* **161**, 22 (1948); J. H. Coon and R. F. Taschek, *Phys. Rev.* **76**, 710 (1949); Hamouda, Halter, and Scherrer, *Helv. Phys. Acta* **24**, 217 (1951); Martin, Burhop, Alcock, and Boyd, *Proc. Phys. Soc. (London)* **A63**, 884 (1950); Griffith, Remley, and Kruger, *Phys. Rev.* **79**, 443 (1950); J. Sanada and S. Yamabe, *Phys. Rev.* **80**, 750 (1950); W. F. Capelhorn and G. P. Rundle, *Proc. Phys. Soc. (London)* **A64**, 546 (1951).

TABLE I. Compilation of target composition and target thickness used and of time integrated neutron flux incident on each target.

A. Single plate camera			
Run number	Target	Surface density of target (mg/cm <sup>2</sup> )	Neutron flux (neutrons/cm <sup>2</sup> )
ND-1	deutero-paraffin	10.9	5.1 × 10 <sup>9</sup>
NP-1	ordinary paraffin	10.4	5.0 × 10 <sup>9</sup>
ND-2	deutero-paraffin	9.8	5.0 × 10 <sup>9</sup>
NP-2	ordinary paraffin	6.04	5.0 × 10 <sup>9</sup>
ND-3	deutero-paraffin	3.20	5.0 × 10 <sup>9</sup>
ND-9	deutero-polyethylene	5.64	4.3 × 10 <sup>9</sup>
ND-10	deutero-polyethylene	7.8	2.0 × 10 <sup>9</sup>
NP-10	polyethylene	7.8	3.8 × 10 <sup>9</sup>
B. Multiplate camera			
Run number	Surface density of front target (mg/cm <sup>2</sup> )	Surface density of back target (mg/cm <sup>2</sup> )	Neutron flux (neutrons/cm <sup>2</sup> )
ND-4	4.73 deutero-paraffin	3.14 ordinary paraffin	2.62 × 10 <sup>9</sup>
ND-5	4.74 ordinary paraffin	2.53 deutero-paraffin	2.62 × 10 <sup>9</sup>
ND-6	2.53 deutero-paraffin	4.73 deutero-paraffin	4.35 × 10 <sup>9</sup>
ND-7	4.73 deutero-paraffin	3.14 ordinary paraffin	2.62 × 10 <sup>9</sup>
ND-8	blank backing	3.16 ordinary paraffin	1.75 × 10 <sup>9</sup>

Externally this part of the collimator has the approximate shape of a pyramid with apex nearest the neutron source. Such a design combines a minimum amount of scattering material (and weight) with a maximum thickness of iron between the detectors and source. Iron was chosen for the basic shielding material since it has a relatively large cross section for inelastic scattering and since the neutrons which are inelastically scattered are greatly degraded in energy.<sup>14</sup> Immediately adjacent to the base of the pyramidal iron section of the collimator is mounted a 6-in. slab of paraffin. A 1¼-in. diameter hole through the paraffin slab is coaxial with the hole through the iron. The primary purpose of the paraffin is further to degrade those neutrons which result from inelastic processes in the iron.

After proceeding down the collimator channel, the neutrons pass into the nuclear plate camera through a 0.003-in. platinum window, thence into the targets at the center of the camera and then out of the camera by way of a second 0.003-in. platinum window. The targets at the center of the camera face in opposite directions, thus permitting simultaneous recording of data from 10° to 170° in the laboratory system. The plane of each target makes an angle of 45° with the axis of the collimator.

Both the deuterium- and hydrogen-containing targets were made by evaporation of paraffin onto 0.007-inch platinum backings.<sup>15</sup> In order to make targets which would be stable in a vacuum, it was found necessary to fractionate the heavy paraffin at 240°C and 0.02 mm Hg, and then to use the higher melting point fraction for the evaporations. The evaporation of the heavy fraction of the deutero-paraffin was carried out at 310°C in a good vacuum (<10<sup>-4</sup> mm Hg before evaporation started). The procedure was to place an appropri-

ate amount of the deutero-paraffin in the bottom of a glass tube ½ in. in diameter and 5 in. long, above which was mounted the platinum backing with all portions except the center ½ in. masked off. The tube containing the deutero-paraffin was then immersed in an oil bath at 310°C and left there until refluxing action ceased. The weight of deutero-paraffin originally placed in the system to give the desired foil thickness was determined to a first approximation by experiments with ordinary paraffin and then determined empirically by trials with deutero-paraffin. The above simple procedure permitted almost complete recovery of that portion of the deutero-paraffin which was not deposited on the target. Also, the initial amount of heavy paraffin required to make the targets was less than 0.5 g.

The target weights were determined with an accuracy of approximately 1 percent on a Mettler Gram-atic balance. After the experiment the targets were reweighed and there was good agreement with the previous weighings. Table I gives the surface densities of the targets used for each run as well as the time-integrated neutron flux incident on the targets. The target facing in the direction of the neutron beam will be designated the front target while that facing in the opposite direction will be designated the back target.

The hydrogen content of the light (ordinary) paraffin and the deuterium content of the heavy paraffin were determined by chemical analyses.<sup>16</sup> The procedure was to oxidize a given weight of paraffin to carbon dioxide and water and then to determine the weights of these combustion products.

The hydrogen content of the light paraffin was determined to be 14.98 ± 0.02 percent by weight. This corresponds to an average chemical formula which is very close to C<sub>22</sub>H<sub>46</sub>. Comparison of the combined weights of the C and H<sup>1</sup>, as determined from the weights of CO<sub>2</sub> and H<sub>2</sub>O, with the original weight of the paraffin indicated a completely negligible amount of high atomic weight impurity.

The analysis of the deutero-paraffin presented some complications due to the presence of an appreciable amount of H<sup>1</sup>. The oxidation of this wax thus yields CO<sub>2</sub>, D<sub>2</sub>O, and H<sub>2</sub>O. In order to determine the deuterium content by the above chemical procedure, it is first necessary to determine the H<sup>1</sup> content. This information is, however, immediately available from the range analyses which were carried out at each angle at which cross-section measurements were made. Each of these range analyses contains a group of tracks corresponding in range to protons knocked on by the incident neutrons. From the number of such protons, the *n-p* cross section and the weight of the target, the H<sup>1</sup> contamination in the heavy wax was determined to be 0.5 to 0.7 percent by weight. By utilizing this

<sup>14</sup> E. R. Graves and L. Rosen, Phys. Rev. **89**, 343 (1953).

<sup>15</sup> The deutero-paraffin was made for us during the war by Texaco. This sample of wax had been prepared by the reduction of carbon monoxide using the Fischer-Tropsch process.

<sup>16</sup> These analyses were carried out for us by A. R. Ronzio of this laboratory.

result along with the results of the chemical analysis one immediately obtains the respective weights of  $D_2O$  and  $H_2O$  from the oxidation of a given weight of heavy wax, and hence the deuterium content which, for the deuterio-wax used, turned out to be  $24.8 \pm 0.4$  percent by weight. From the sum of the weights of  $CO_2$ ,  $D_2O$ , and  $H_2O$  and the uncertainties in their values it is again possible to place an upper limit on heavy impurities. If, for example, one assumes a contaminant with atomic weight 16, it is deduced that there must certainly be less than 0.3 atomic percent of such an impurity. If the impurity is heavier the above upper limit is correspondingly less.

The nuclear plates (Ilford C-2) were placed around the periphery of the camera in a plane perpendicular to the plane of the targets, so that the longitudinal axes of the plates lay on radii passing through the vertical axis of the target support. The long range of the recoil particles and the large angle these particles made with the emulsion surfaces made it desirable to use  $400\mu$  emulsions in the forward  $50^\circ$ ;  $200\mu$  emulsions proved adequate elsewhere.

The procedure for making a run, after loading the camera, was to evacuate the camera for a period of 1 hour before starting up the Cockcroft-Walton. The vacuum system contained a liquid air trap for the purpose of desiccating the emulsion. Pumping on the camera was maintained for the duration of the run, which usually lasted about 14 hours. When the run was completed, the plates were transferred to a light-tight box for transportation to the darkroom. The loading and unloading of the camera was accomplished under a light-tight tent equipped with a Wratten No. 2 safelight.

All plates were processed by a combination of the temperature development method<sup>17</sup> and the two solution technique.<sup>18</sup> For the  $400\mu$  plates the only significant departure from the procedure described by Stiller *et al.*<sup>17</sup> was substitution of two solutions for the amidol developer. For the  $200\mu$  plates only the soak and developer solutions were at low temperature. In this modified procedure, the  $200\mu$  plates are first soaked in distilled water for 1 hour at  $5^\circ C$ . They are then placed consecutively in solution A for 50 minutes and in solution B for 50 minutes, both solutions being maintained at  $5^\circ C$ . The formulas for solution A and B are given in reference 18.

Upon removal from solution B the plates are placed, emulsion side up, on toweling at a room temperature of  $22^\circ C$ , and permitted to remain so for 20 minutes. The plates are now placed consecutively in a stop bath of 2 percent acetic acid for 20 minutes, neutral hypo for approximately 5 hours (the hypo being changed

every hour), acid hypo for  $\frac{1}{2}$  hour and, finally, into wash water for 2 hours. The acetic acid, hypo, and wash water are all maintained at approximately  $22^\circ C$ . The surface silver is rubbed off with chamois or a finger when the plates are removed from the stop bath. The plates are placed, still in Lucite holders which keep them horizontal with emulsion side up, in a room at  $22^\circ C$  and permitted to dry.

The plates were scanned under magnifications from 450 to 900 diameters, using apochromatic oil immersion objectives and compensating eyepieces. Tracks of length less than  $100\mu$  were measured with a calibrated eyepiece graticule, whereas tracks of length greater than  $100\mu$  were measured by means of a micrometer screw and graduated drum assembly built by Erb and Gray of Los Angeles. The device makes possible the precise and rapid measurement of long tracks. (A  $1000\mu$  projection can be measured to an accuracy of  $\pm 3$  microns.) The orientation of a given track was determined from its dip into the emulsion and its displacement in the horizontal plane. The latter measurement was made with the eyepiece graticule while the former was made with the fine focus screw. The dip was corrected for shrinkage of the emulsion. Each plate was divided into nine areas, each 1 cm long and 2 to 4 mm wide. Two to eight such areas of 20 to 40 mm<sup>2</sup> were scanned on each plate. The size and position of the plate area analyzed determine the solid angle subtended at the target, while the position of this area and the position of the plate in the camera determine the angle of observation in the laboratory system with respect to the direction of the neutron beam. (The angular resolution varied from  $10^\circ$  at  $45^\circ$  to  $5^\circ$  at  $20^\circ$ .) Tracks whose directions were inconsistent with the radiator-detector geometry were considered to be spurious. Such tracks were due to a variety of factors such as protons from the nuclear emulsion being knocked on by background neutrons, ( $n, p$ ) reactions in the 0.010-in. gold lining of the camera, ( $n, p$ ) reactions in the residual gas and water vapor in the camera, and, at small angles, protons produced by neutron interactions outside the camera with sufficient energy and in the proper direction to enter the camera via the window facing the collimator. Such elimination from consideration of tracks on the basis of direction was further justified by background runs made with a blank target. Since the solid angle of acceptance of tracks was only about  $10^{-3}$  of the total solid angle, this criterion for excluding spurious tracks was of considerable help in coping with the background tracks which are, to a greater or lesser extent, always present in neutron experiments.

The problem of determining the differential cross sections for the  $n-d$  and  $n-p$  elastic scattering involved the extraction of the peaks of  $n-d$  and  $n-p$  recoils due to 14.1-Mev neutrons from the measured range distributions. The above procedure for eliminating most of the background plus the use of nearly monoenergetic

<sup>17</sup> Dilworth, Occhialini, and Vermaesen, Bull. centre phys. nucléaire univ. libre Bruxelles, Belgium No. 13a (February, 1950); Bonetti, Dilworth, and Occhialini, Bull. centre phys. nucléaire univ. libre Bruxelles, Belgium No. 13b (March, 1951); Stiller, Shapiro, and O'Dell, Phys. Rev. **85**, 712 (1951).

<sup>18</sup> M. Blau and J. A. De Felice, Phys. Rev. **74**, 1198 (1948).

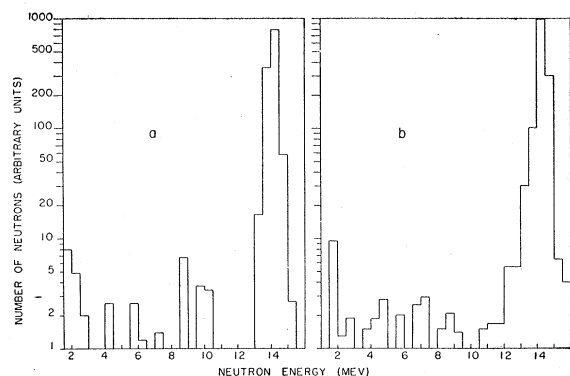


FIG. 2. Neutron spectrum incident on target.

neutrons made this determination quite straightforward and precise.

One objective of these experiments was to determine the cross section for the reaction  $D(n, 2n)H^1$ . It was therefore necessary to have precise information on the energy distribution of the neutrons striking the deuterium target, since degraded neutrons can produce knock-on deuterons which, at any given angle, will have a range less than that of the deuterons elastically scattered by 14-Mev neutrons and may therefore be confusable with protons from deuteron breakup. After a small background correction has been made on the basis of the blank target run, the energy spectrum of the neutrons incident on the target is determined from the  $n$ - $p$  scattering experiment by the following procedure.

The distribution in range of the recoil protons, at any given angle, is converted to a proton energy distribution by using the appropriate range-energy curves; the proton energy distribution is in turn con-

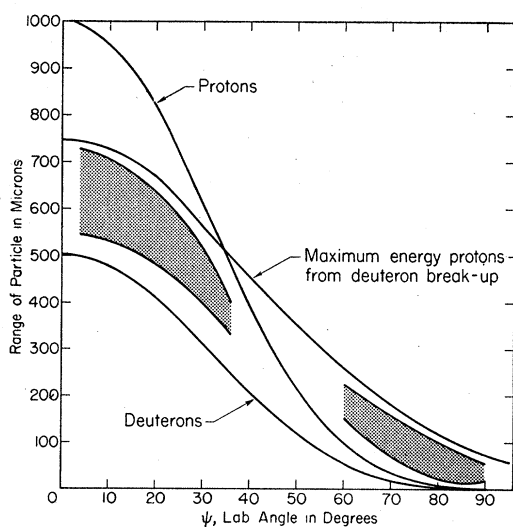


FIG. 3. Range versus angle for charged particles arising from the interaction of 14.1-Mev neutrons with deuterons. The shaded area indicates the region in which protons from deuteron disintegrations can be resolved on the basis of their range.

verted into a neutron energy distribution by the relation  $E_p = E_n \cos^2 \psi$ , where  $E_p$  = observed proton energy,  $E_n$  = inferred neutron energy, and  $\psi$  is the average angle between the directions of the incident neutron beam and the recoil proton. Finally the relative number of neutrons in each energy interval is divided by the neutron-proton scattering cross section for the mean energy of that interval. The resultant histogram represents the neutron spectrum incident on the target. Two examples are shown in Figs. 2a and 2b. Figure 2a is based on data taken at  $13^\circ$  with respect to the neutron beam direction; Fig. 2b is based on the combined data taken at 15 angles from  $15^\circ$  to  $40^\circ$ . The large apparent spread in energy of the main neutron group in Fig. 2b is the result of a decrease in measuring resolution on account of the following two factors: One, at large angles the stopping power of the target is no longer small compared to the range of the scattered protons; Two, for large values of  $\psi$ , relatively small variations in  $\psi$  (induced by the angular resolution) are reflected as large variations in  $\cos^2 \psi$ , the factor which determines the neutron energy corresponding to a given proton energy. The blank target background correction is less than 2 percent of the proton group which corresponds to the main neutron group in each figure.

In experiments involving the neutron-deuteron interaction it is essential to distinguish between recoil deuterons, recoil protons from the hydrogen contamination of the deuterio-paraffin, and protons from deuteron breakup. Figure 3 shows the variation of range with laboratory angle for the particles from the first two reactions and for the maximum energy protons from the third reaction. This latter is calculated on the assumption that the two neutrons go off in the same direction and with equal velocities. It is apparent that the recoil protons from hydrogen contamination in the heavy paraffin are always separable from the recoil deuterons but not from the highest energy disintegration protons. However, once the degree of contamination is firmly established at angles where adequate separation in range does exist, a correction can be made at other angles on the basis of the hydrogen content of the deuterio-paraffin and the differential  $n$ - $p$  scattering cross section for 14-Mev neutrons. The correction for deuterons knocked on by degraded neutrons is much more difficult to evaluate. Since such low energy deuteron recoils are indistinguishable, in the emulsion, from protons of the same range, it is necessary to make a correction for these tracks. The correction was calculated on the basis of the neutron spectrum incident on the target (Fig. 2b) and the known differential cross sections with respect to energy and angle for  $n$ - $d$  and  $p$ - $d$  scattering. The  $p$ - $d$  scattering data were used in addition to  $n$ - $d$  scattering data since insufficient  $n$ - $d$  scattering data are available. For the purpose of these calculations the differential cross section at energy  $E$  for  $n$ - $d$  scattering is assumed equal to the differential cross section for  $p$ - $d$  scattering at

energy ( $E+0.7$ ) Mev. (The  $p$ - $d$  scattering data were used only at large angles where Coulomb scattering would be unimportant.)

To obtain data at laboratory angles smaller than  $10^\circ$  and to lend additional credence to the cross-section values obtained at angles investigated by means of the arrangement shown in Fig. 1, we have utilized the target-detector geometry shown schematically in Fig. 4 to measure cross-section values for  $n$ - $d$  scattering and deuteron breakup at  $2^\circ$ ,  $13^\circ$ ,  $15^\circ$ , and  $24.4^\circ$ . This geometry does not involve use of a neutron collimator. The agreement, on an absolute scale, of the data from the single plate camera shown in Fig. 4 with that from the multiplate camera is a welcome check.

In addition to making runs with a single plate camera and with different target thicknesses as well as with a blank target in the multiplate camera, the following checks were made to establish the fact that the various range groups of tracks observed actually came from the target.

(a) A plot was made of the number of tracks observed *versus* projected angle in the horizontal plane. A similar plot was made with respect to the angle in

TABLE II. Summary of  $n$ - $p$  scattering data.

$\Omega$ c. m. angle (degrees)	$\sigma(\Omega)$ (barns/ steradian)	Statistical error (percent)
154.5	0.0547	2.6
146.6	0.0540	3.5
131.7	0.0533	3.8
114.7	0.0518	3.5
100.5	0.0513	4.7
84.1	0.0533	4.4
66.9	0.0493	5.0
48.0	0.0507	4.6

the vertical plane. The variation of number of tracks with angle was determined to be consistent with the position of the area of the plate analyzed and the size of target as seen by this area.

(b) Areas at various distances from the target were analyzed to determine whether the number of tracks of each range group was proportional to the solid angle subtended at the target by the plate area analyzed.

In the  $n$ - $d$  experiment grain counts were made, at several angles, of tracks in the elastically scattered range group, and between the deuteron peak and the range group caused by knock-on protons from  $H^1$  contamination in the deuterio-paraffin. The tracks between the deuteron and proton peaks were thus established to be protons rather than deuterons, a conclusion which, at forward angles, is unavoidable on the basis of energy considerations.

### III. RESULTS AND DISCUSSION

#### (A) $n$ - $p$ Scattering

The differential cross section for  $n$ - $p$  scattering in the laboratory system is determined by the relation

$$\sigma(\psi) = N_p R^2 / n_0 N A \sin\phi, \quad (1)$$

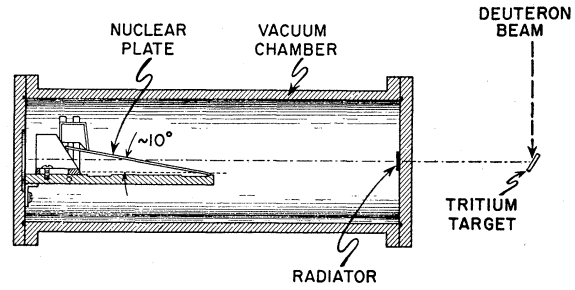


FIG. 4. Schematic drawing of single plate camera.

where

$\sigma(\psi)$  = cross section per unit solid angle in the laboratory coordinate system at angle  $\psi$ ,

$\psi = \arccos(\cos\theta \cos\phi)$  (see Fig. 1),

$A$  = area of plate scanned,

$N_p$  = number of protons of proper length and direction counted in  $A$ ,

$R$  = distance from center of target to center of  $A$ ,

$\phi$  = angle between plane of emulsion, (i.e., of  $A$ )

and line from center of  $A$  to center of target

= angle of dip into unprocessed emulsion,

$n_0$  = number of hydrogen atoms in the target

= weight of target in grams  $\times 0.1498 \times 6.025 \times 10^{23}$ , and

$N$  = number of neutrons per  $\text{cm}^2$  that passed through the target.

In order to convert  $\sigma(\psi)$  to the differential cross section in the c.m. system one simply multiplies by the factor giving the ratio of solid angles in the laboratory and c.m. systems. This factor is  $1/(4 \cos\psi)$ . The c.m. angle  $\Omega$  which corresponds to a laboratory angle  $\psi$  is  $\Omega = 180^\circ - 2\psi$ .

Figure 5 and Table II give the results, in the center-of-mass system, for the angular distribution of 14.1-Mev neutrons scattered by protons. Although these results are not inconsistent with spherical symmetry, a slight asymmetry is by no means ruled out. The errors

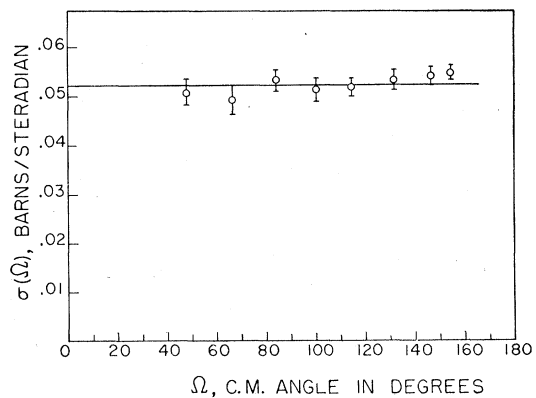


FIG. 5. Angular distribution of 14.1-Mev neutrons scattered by protons.

TABLE III. Summary of  $n$ - $d$  scattering data.

$\psi$ lab angle (degrees)	$\sigma(\psi)$ (barns/ steradian)	$\Omega$ c.m. angle (degrees)	$\sigma(\Omega)$ (barns/ steradian)	Statistical error (percent)	Estimated error arising from confusable protons (percent)
<sup>a</sup> 2.0	0.440	176.0	0.110	3.4	0
11.0	0.308	158.0	0.0795	5.9	0
12.4	0.228	155.2	0.0585	5.0	0
<sup>a</sup> 13.0	0.230	154.0	0.0590	6.0	0
14.0	0.196	152.0	0.0505	5.8	2
14.5	0.208	151.0	0.0537	5.1	2
<sup>a</sup> 15.0	0.189	150.0	0.0489	8.0	3
17.5	0.125	145.0	0.0328	7.1	5
18.3	0.113	143.4	0.0298	6.2	6
20.8	0.0712	138.4	0.0191	9.2	7
22.9	0.0553	134.2	0.0150	8.3	7
23.6	0.0455	132.8	0.0123	9.7	7
<sup>a</sup> 24.4	0.0410	131.2	0.0113	12.0	10
26.7	0.0390	126.6	0.0110	8.5	7
29.3	0.0401	121.4	0.0115	8.5	7
30.3	0.0398	119.4	0.0115	6.5	7
32.8	0.0399	114.4	0.0122	6.4	7
34.8	0.0433	110.4	0.0132	8.4	6
38.6	0.0530	102.8	0.0171	5.7	4
46.7	0.0970	86.6	0.0355	5.1	4
51.2	0.106	77.6	0.0422	5.5	4
52.4	0.117	75.2	0.0477	5.4	4
55.3	0.119	69.4	0.0520	7.7	4
57.8	0.128	64.4	0.0598	3.9	5
65.5	0.139	49.0	0.0841	6.5	5
67.0	0.134	46.0	0.0859	10.8	5

<sup>a</sup> Single plate camera data.

indicated in the figure and table are standard deviations due to statistical uncertainties alone. The standard error arising from the evaluation of  $R$ ,  $A$ ,  $\phi$ ,  $n_0$ , and  $N$  in Eq. (1) is approximately 5 percent. The most probable value of the ratio of the cross section in the region of  $130^\circ$  to  $155^\circ$  to the cross section in the angular region of  $65^\circ$  to  $105^\circ$  is  $1.04 \pm 0.05$ .

Our angular distribution is in quite good agreement with the angular distribution of Barschall and Taschek. The total cross section obtained from our data, by assuming spherical symmetry, is  $0.66 \pm 0.05$  barn. The value obtained by transmission measurements at this energy is  $0.689 \pm 0.005$  barn.<sup>19</sup>

### (B) $n$ - $d$ Interaction

The method of calculating the differential cross section in the center-of-mass system as a function of angle for  $n$ - $d$  elastic scattering is identical with that outlined for the  $n$ - $p$  scattering.  $n_0$  was determined from the weight and composition of the deuterio-paraffin.

Figure 6 and Table III give the results of the angular distribution measurements for  $n$ - $d$  elastic scattering. Figure 6 gives all of the points obtained in the various runs. The large degree of scattering of the points shown is due chiefly to statistical fluctuations. Table III gives the weighted averages of the cross-section values

<sup>19</sup> Poss, Salant, Snow, and Yuan, Phys. Rev. **87**, 11 (1952).

displayed in Fig. 6. In addition to statistical inaccuracies there exist errors attributable to the following:

(a) Uncertainties in the evaluation of the background in the range group of the elastically scattered deuterons. The portion of this background caused by  $D(n, 2n)H^1$  was, of course, not present in the  $n$ - $p$  problem; estimates of these errors are given in column six of Table III.

(b) Geometrical factors ( $R^2$ ,  $A$ ,  $\phi$ , Eq. (1)): 3 percent.

(c) Number of deuterium atoms in target [ $n_0$ , Eq. (1)]: 3 percent.

(d) Number of neutrons per  $\text{cm}^2$  passing through target [ $N$ , Eq. (1)]: 3.5 percent.

The 14-Mev neutron flux at the target was calculated on the basis of the number of neutrons generated in the source, as given by the alpha-particle counter and the distance between source and target. No correction was made for a possible contribution to the flux at the target by elastic scattering in the walls of the collimator channel. Experiments which we have performed to date indicate that this effect is less than 2 percent. However, if such a systematic error did exist it would mean that all the cross-section values obtained from the multiplate camera are too high by the amount of this error.

Our  $n$ - $d$  elastic scattering results are in reasonably good agreement with the most recent results of Coon and Taschek.<sup>20</sup> There still appears to be a discrepancy in the region of the minimum where the present results are lower than those of Coon and Taschek by an amount which is somewhat outside the combined errors. This difference, however, may be due to the fact that we have corrected our data for the presence of those protons from deuteron breakup which fall into the range group of elastically scattered deuterons. The

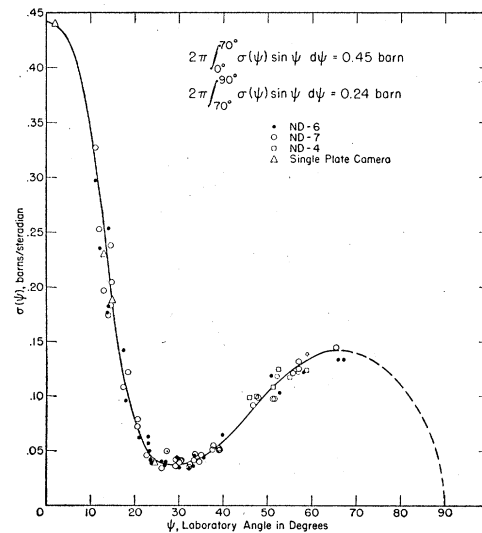


FIG. 6. Angular distribution of deuterons knocked on by 14.1-Mev neutrons.

<sup>20</sup> J. H. Coon (private communication).

correction was made on the basis of the shape of the range distribution of the charged particles recorded above and below the elastically scattered deuteron range group at each angle.

It is rather difficult to compare the data of Griffith, Remley, and Kruger<sup>11</sup> with the present data since theirs were taken at a lower energy and their cross-section scale is not absolute. However, if one normalizes the Illinois data to our own at 90°, the agreement is as good as one might expect, especially since their elastic scattering cross sections include a contribution from the cross section for deuteron breakup. This contribution is in the proper direction and probably of sufficient magnitude to account for any discernible disagreement in the region of the minimum.

Figure 7 compares our results with the theoretical predictions of Buckingham, Hubbard, and Massey<sup>5</sup> on the assumption of symmetrical exchange type forces. The disagreement may well be due to the fact that the theoretical calculations assumed no contribution from relative angular momentum states above  $l=2$  ( $d$  scattering). A detailed analysis of these data has recently been carried out by Christian and Gammel.<sup>21</sup> Their calculated  $n-d$  angular distribution at 14.1-Mev neutron energy is in excellent agreement with the present experimental results.

In Figs. 6 and 7, the experimental angular distributions have been extrapolated to zero degrees and the curves integrated. The average total cross section for elastic scattering arrived at in this manner is  $0.67 \pm 0.10$  barn. This value is significantly lower than the total cross section value of 0.802 barn obtained from transmission measurements.<sup>19</sup> The rather large difference appears to be good evidence for the existence of an appreciable cross section for deuteron disintegration at this energy. There is, moreover, additional evidence

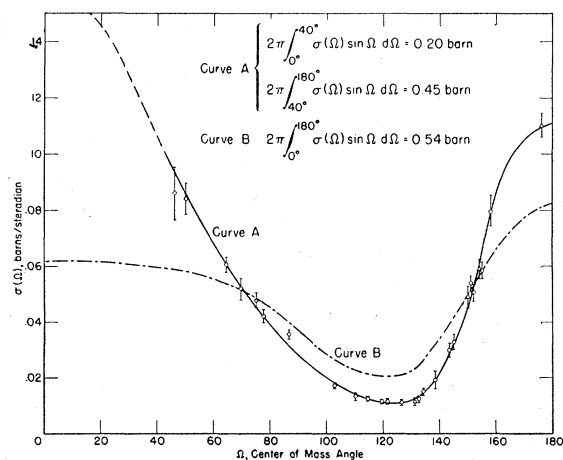


FIG. 7. Comparison of experimental and theoretical angular distributions of 14.1-Mev neutrons scattered by deuterons.

<sup>21</sup> R. S. Christian and J. L. Gammel (following paper), Phys. Rev. **91**, 100 (1953).

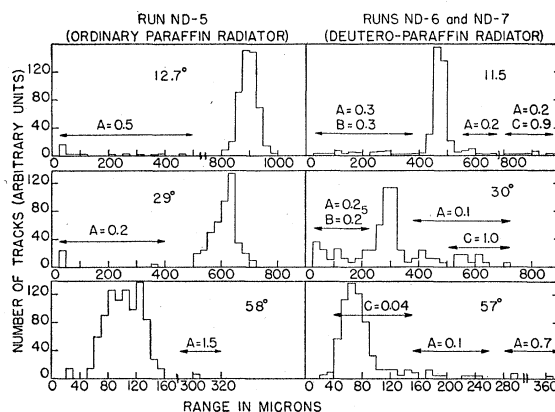


FIG. 8. Distribution in range of charged particles from  $n-d$  and  $n-p$  interactions at various angles.

for this process based on the observation of the protons which result from such breakup.

Figure 8 shows the distributions in range of all the charged particles from the  $n-d$  and  $n-p$  interactions at various angles. The values assigned to  $A$  in this figure give the fraction of the tracks, in the range interval indicated, which must be subtracted on the basis of the blank target run for the forward angles and *Run ND-7* (Table I) for the backward angles.<sup>22</sup> It is apparent, at least qualitatively, that the histograms of the charged particles from the  $n-d$  interaction show more tracks outside of the range groups corresponding to elastic scattering than do the corresponding  $n-p$  histograms. In particular, those tracks which fall between the range groups of elastically scattered deuterons and protons, cannot be due to deuterons elastically scattered by the primary beam of 14.1-Mev neutrons. The tracks which appear below the range group of elastically scattered deuterons can, however, be due to deuterons elastically scattered by degraded neutrons and corrections must accordingly be applied. The values assigned to  $B$  in Fig. 8 give the fraction of the plotted tracks, in the range interval indicated, which is deduced to be due to deuterons elastically scattered by degraded neutrons.  $C$  designates the range interval within which one expects to find tracks of knock-on protons from the hydrogen in the target. The values assigned to  $C$  refer to the fraction of tracks in the designated range interval which one calculates to come from such scatterings on the basis of a 0.05 ratio of  $H^1$  to  $H^2$  atoms. These corrections were made on the basis of what is known about  $n-d$  and  $p-d$  elastic scattering cross sections as a function of angle and energy. Figure 9 gives the angular distributions used for these corrections. In energy regions where no data are available, a log-log extrapolation of the data illustrated in Fig. 9

<sup>22</sup> At 11° the relatively large number of background tracks of range greater than 500 $\mu$  were determined to be caused by a small amount of grease on the outside of the front window. At larger angles such tracks were eliminated from consideration on the basis of their direction.

was used. The dotted curve is an example of the results of such an extrapolation for 14.1-Mev  $n$ - $d$  scattering.

Figure 10 shows, in a semiquantitative manner, the deduced angular distribution for emission of protons from deuteron breakup. The large errors arise from the uncertainty in the background correction. It is to be noted that tracks of range less than  $25\mu$  were not considered since it was felt that the measurement of their orientation with respect to the target could not be made with sufficient precision. This limitation, together with energy loss in the target, implies that protons emitted with less than approximately 2-Mev energy would not be counted. A serious source of error in the assignment of differential cross sections for deuteron breakup arises from the possibility that unknown contaminants might give rise to protons from ( $n, p$ ) reactions which would be indistinguishable, energywise, from deuteron breakup protons. The chief sources of such contaminants are probably the catalysts used in the preparation of the wax. To check further on this point we repeated a number of the single-plate camera runs using deuterio-polyethylene as a target rather than deuterio-paraffin. For the background run

we used ordinary polyethylene prepared by exactly the same process.<sup>23</sup> The preparation of the polyethylene involved different catalysts from those used in the preparation of the heavy wax. The results for both elastic scattering and deuteron disintegration were independent of the target used and this fact, together with the very reasonable variation with angle of the range distribution of the disintegration protons, gives us considerable confidence that contaminants are not causing serious difficulty.

The total cross section for deuteron breakup with the emission of protons of energy above 2 Mev is deduced, from the data given in Fig. 10, to be  $53 \pm 15$  millibarns. This value does not appear to be in violent disagreement with the total cross section for this process as deduced from the data of other investigators. Coon and Taschek,<sup>11</sup> for example, report a maximum value of 50 millibarns for the cross section for the disintegration process over the range from  $0^\circ$  to  $80^\circ$  in the laboratory system.

Agno, Amaldi, Bocciarelli, and Trabacchi<sup>24</sup> estimated a cross section for this process of 40 to 90 millibarns; while Griffith, Remley, and Kruger<sup>11</sup> also

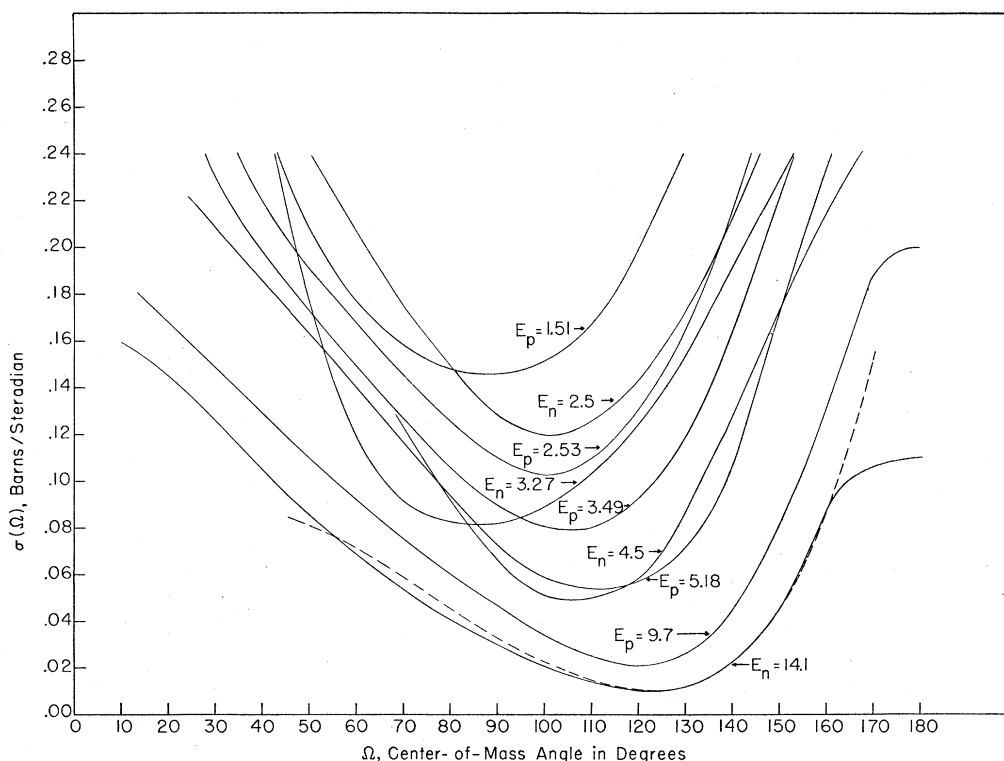


FIG. 9. Experimental angular distributions for  $n$ - $d$  and  $p$ - $d$  scattering. The dashed curve is a log-log extrapolation to 14-Mev neutron energy of the following lower energy data:  $E_p = 1.51, 2.53,$  and  $3.49$  Mev—Sherr, Blair, Kratz, Bailey, and Taschek, Phys. Rev. **72**, 662 (1947);  $E_n = 2.5$  Mev—R. K. Adair (private communication);  $E_n = 3.27$  Mev—I. Hamouda and G. de Montmollin, Phys. Rev. **83**, 1277 (1951);  $E_n = 4.5$  Mev—E. Wantuch, Phys. Rev. **84**, 169 (1951);  $E_p = 5.18$  Mev—L. Rosen and J. C. Allred, Phys. Rev. **82**, 777 (1951);  $E_p = 9.7$  Mev—Allred, Armstrong, Bondelid, and Rosen, Phys. Rev. **88**, 433 (1952);  $E_n = 14.1$  Mev—present data.

<sup>23</sup> The polyethylene was also prepared for us by A. R. Ronzio.

<sup>24</sup> Agno, Amaldi, Bocciarelli, and Trabacchi, Phys. Rev. **71**, 20 (1947).

observed a significant probability for this reaction at 12- to 13-Mev neutron energy. All the above data, present experiment included, indicate a lower cross section for deuteron breakup, by an order of magnitude, than is theoretically predicted.<sup>25</sup>

It is interesting to speculate concerning the reason that more high energy protons are not emitted in the forward direction. It may be that this mode of disintegration is, to some extent, inhibited by the Pauli exclusion principle, for if the incident neutron transfers most of its energy to the proton in the deuteron, the two remaining neutrons might well be left in an *S*-state of orbital angular momentum and this is, of course, only possible in the case of antiparallel spins.

The authors are indebted to the entire staff of the nuclear plate laboratory for the very careful plate analysis work upon which this report is based. We wish also to express our appreciation to Rexine Booth, Juanita Gammel, and Leona Stewart for their assistance in the reduction and compilation of the data and to

<sup>25</sup> B. H. Bransden and E. H. Burhop, Proc. Phys. Soc. (London) **A63**, 1337 (1950).

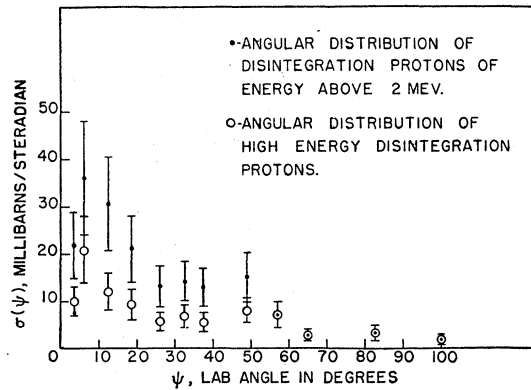


FIG. 10. Angular distribution for emission of protons from deuteron breakup. The dots represent the angular distribution of all disintegration protons of energy greater than 2 Mev; the open circles represent the angular distribution of only those protons whose range is greater than the range of the elastically scattered deuterons at the same angle.

Leona Stewart for her very considerable help in the preparation of the manuscript.